Remote Sensing of Environment 163 (2015) 270–285

Contents lists available at ScienceDirect

Remote Sensing of Environment

journal homepage: www.elsevier.com/locate/rse

Assessment of five global satellite products of fraction of absorbed photosynthetically active radiation: Intercomparison and direct validation against ground-based data

Xin Tao [a,*], Shunlin Liang [a,b], Dongdong Wang [a]

[a] Department of Geographical Sciences, University of Maryland, College Park, MD 20742, USA
[b] State Key Laboratory of Remote Sensing Science, School of Geography, Beijing Normal University, Beijing 100875, China

ARTICLE INFO

Article history:
Received 11 July 2014
Received in revised form 28 March 2015
Accepted 29 March 2015
Available online 14 April 2015

Keywords:
Fraction of absorbed photosynthetically active radiation
Intercomparison
Direct validation
MODIS
MISR
MERIS
SeaWiFS
GEOV1

ABSTRACT

The fraction of absorbed photosynthetically active radiation (FAPAR) is a critical input parameter in many climate and ecological models. The accuracy of satellite FAPAR products directly influences estimates of ecosystem productivity and carbon stocks. The targeted accuracy of FAPAR products is 10%, or 0.05, for many applications. It is important to evaluate satellite FAPAR products and understand differences between the products to effectively use them in carbon cycling models. In this study, five global FAPAR products, namely MODIS, MISR, MERIS, SeaWiFS, and GEOV1 are intercompared over different land covers and directly validated with ground-based measurements at VAlidation of Land European Remote sensing Instruments (VALERI) and AmeriFlux sites. Intercomparison results show that MODIS, MISR, and GEOV1 agree well with each other and so do MERIS and SeaWiFS, but the difference between these two groups can be as large as 0.1. The temporal trends of these products agree better with each other in the Northern Hemisphere than in the Southern Hemisphere. The trends in the Northern Hemisphere are similar to those globally. However, the conclusions from the northern hemispheric scale could not be extended to the global scale for land covers such as savannahs and broadleaf evergreen forests. The differences between the products are consistent throughout the year over most of the land cover types, except over the forests, because of the different assumptions in the retrieval algorithms and the differences between green and total FAPAR products over forests. Direct validation results show that MERIS, MODIS, MISR, and GEOV1 FAPAR products have an uncertainty of 0.14 when validating with total FAPAR measurements, and 0.09 when validating with green FAPAR measurements. Overall, current FAPAR products are close to, but have not fulfilled, the accuracy requirement, and further improvements are still needed.

1. Introduction

The fraction of absorbed photosynthetically active radiation (FAPAR) is the fraction of incoming solar radiation in the spectral range of 400 nm to 700 nm that is absorbed by plants (Liang, Li, & Wang, 2012). FAPAR is one of the 50 Essential Climate Variables (ECVs) recognized by the UN Global Climate Observing System (GCOS, 2011). FAPAR is a critical input parameter in the biogeophysical and biogeochemical processes described by many climate and ecological models (e.g., Community Land Model, Community Earth System Model, and crop growth models) (Bonan et al., 2002; Kaminski et al., 2012; Maselli, Chiesi, Fibbi, & Moriondo, 2008; Tian et al., 2004).

The accuracy of the satellite FAPAR products directly influences estimates of ecosystem productivity and carbon stocks. A relative accuracy of 10%, or absolute accuracy of 0.05, in FAPAR is considered acceptable in agronomical and other applications (GCOS, 2011). MODIS Collection 4 FAPAR product is validated with ground-based measurements in early studies (Baret et al., 2007; Fensholt, Sandholt, & Rasmussen, 2004; Huemmrich, Privette, Mukelabai, Myneni, & Knyazikhin, 2005; Olofsson & Eklundh, 2007; Steinberg, Goetz, & Hyer, 2006; Turner et al., 2005; Weiss, Baret, Garrigues, & Lacaze, 2007; Yang et al., 2006). The improved performance of Collection 5 over Collection 4 LAI/FAPAR products is demonstrated before the public release by Shabanov et al. (2005). Recently, the MODIS Collection 5 FAPAR product is assessed or compared with other products and has been shown to improve accuracy over Collection 4 from 0.2 to 0.1 (Baret et al., 2013; Camacho, Cemicharo, Lacaze, Baret, & Weiss, 2013; Martinez, Camacho, Verger, Garcia-Haro, & Gilabert, 2013; McCallum et al., 2010; Pickett-Heaps et al., 2014). An intermediate MODIS FAPAR Collection 4.1 product fixes the bug that existed in Collection 4, and its performance is assessed to have improved over Collection 4 but not as good as Collection 5 (Seixas, Carvalhais, Nunes, & Benali, 2009; Serbin, Ahl, & Gower, 2013). The MERIS FAPAR product has been assessed or compared with other FAPAR products and validated to show an accuracy

* Corresponding author. Tel.: +1 301 405 4538; fax: +1 301 314 9299.
E-mail address: xtao@umd.edu (X. Tao).

http://dx.doi.org/10.1016/j.rse.2015.03.025
0034-4257/

Table 1
The AmeriFlux and VALERI experimental sites used in this study.

Site	State, Country	Latitude (°)	Longitude (°)	Land Cover
Mead Irrigated	Nebraska, US	41.1651	−96.4766	Crops
Mead Irrigated Rotation	Nebraska, US	41.1649	−96.4701	Crops
Mead Rainfed	Nebraska, US	41.1797	−96.4396	Crops
Bartlett	New Hampshire, US	44.0646	−71.2881	Deciduous broadleaf forests
Laprida	Argentina	−36.9904	−60.5527	Grass
Camerons	Australia	−32.5983	116.2542	Evergreen broadleaf forests
Gnangara	Australia	−31.5339	115.8824	Deciduous broadleaf forests
Sonian forest	Belgium	50.7682	4.4111	Needleleaf forests
Donga	Benin	9.7701	1.7784	Grass
Turco	Bolivia	−18.2395	−68.1933	Shrubland
Larose	Canada	45.3805	−75.2170	Needleleaf forests
Concepción	Chile	−37.4672	−73.4704	Deciduous needleleaf forests
Zhangbei	China	41.2787	114.6878	Grass
Les Alpilles	France	43.8104	4.7146	Crops
Larzac	France	43.9375	3.1230	Grass
Nezer	France	44.5680	−1.0382	Needleleaf forests
Plan-de-Dieu	France	44.1987	4.9481	Crops
Puéchabon	France	43.7246	3.6519	Mediterranean forests
Sud-Ouest	France	43.5063	1.2375	Crops
Counami	French Guiana	5.3471	−53.2378	Evergreen broadleaf forests
Demmin	Germany	53.8921	13.2072	Crops
Gilching	Germany	48.0819	11.3205	Crops
Hombori	Mali	15.3310	−1.4751	Grass
Haouz	Morocco	31.6592	−7.6003	Crops
Wankama	Niger	13.6450	2.6353	Grass
Fundulea	Romania	44.4061	26.5831	Crops
Barrax	Spain	39.0570	−2.1042	Crops

The first four sites are AmeriFlux sites, others are VALERI sites.

of 0.1 to 0.12 (D'Odorico et al., 2014; Gobron et al., 2008; Martinez et al., 2013; Pickett-Heaps et al., 2014; Seixas et al., 2009). The Sea-Viewing Wide Field-of-View Sensor (SeaWiFS) FAPAR product has been compared with other FAPAR products and evaluated to have an accuracy of 0.1 to 0.23 in the studies by Wang et al. (2001), Gobron et al. (2006), McCallum et al. (2010), Camacho et al. (2013), and Pickett-Heaps et al. (2014). The GEOV1 FAPAR is intercompared against MODIS Collection 5 and SeaWiFS products and validated to have the best performance with an accuracy of 0.08 (Baret et al., 2013; Camacho et al., 2013). However, few studies have evaluated the Multi-Angle Imaging SpectroRadiometer (MISR) FAPAR product (Hu et al., 2007). Currently, no intercomparison studies of MISR FAPAR product and other FAPAR products exist. The intercomparison of the products at various scales would help to understand and reduce large systematic biases among the magnitudes of existing products. In consideration of the need to evaluate current FAPAR products, this study focuses on a comprehensive evaluation of the performances of MISR, MODIS, SeaWiFS, MERIS, and GEOV1 FAPAR products at the global scale.

The remainder of this paper is organized as follows. Section 2 presents the satellite FAPAR products and the validation data as well as the data processing and ground-based measurement methods. Section 3 intercompares FAPAR products globally and over different land cover types. Section 4 directly validates the FAPAR products with ground-based measurements. The findings are discussed and concluded in Sections 5 and 6, respectively.

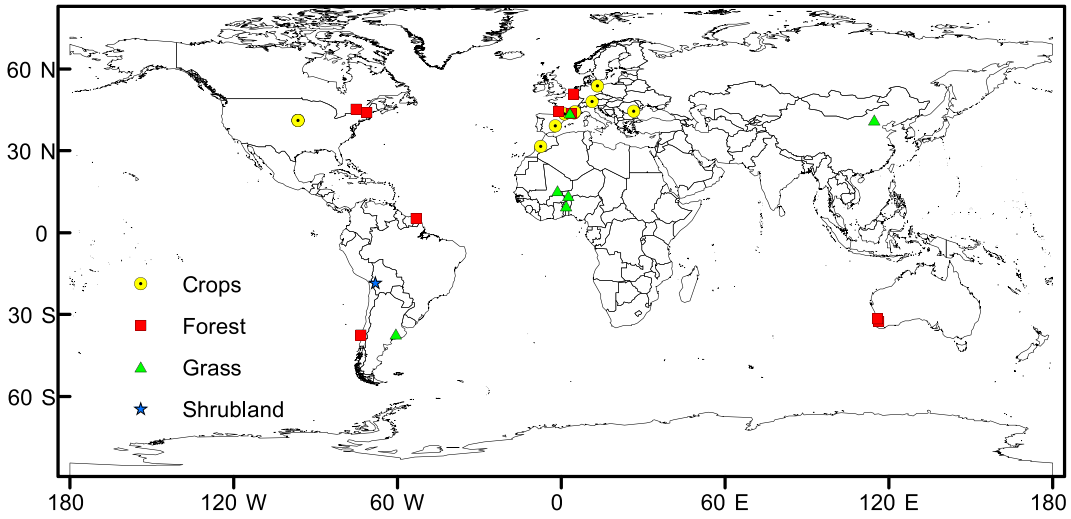

Fig. 1. The distribution of the 27 VALERI and AmeriFlux sites. There are 3 AmeriFlux and 3 VALERI sites close to each other, which may not be distinguishable from each other at a global scale here.

Table 2
The characteristics of the satellite FAPAR products used in this study.

FAPAR Product	Temporal Coverage	Temporal Resolution	Spatial Resolution	Projection	Algorithm
MODIS MOD15 (C5) (WWW3)	Feb 2000–	8 days	1 km	Sinusoidal	Look up table method built on 3D stochastic radiative transfer model for different biomes (Myneni et al., 2002).
MISR (L3/L2) (WWW4)	Feb 2000–	1 month/equator: 9 days, polar: 2 days	0.5°/1 km	Plate-carrée (geographic)/Space Oblique Mercator	Radiative transfer (RT) model with inputs of LAI and soil reflectance without assumptions on biomes (Knyazikhin et al., 1998).
GEOV1 (WWW5)	Dec 1998–	10 days	1/112°	Plate-carrée	Neural network to relate the fused products to the top of canopy SPOT/VEGETATION reflectance (Baret et al., 2013).
MERIS (L3/L2) (WWW6)	Apr 2002–	1 month/daily	0.5°/1 km	Plate-carrée/sinusoidal	Polynomial formula based on 1D RT model (Gobron, Pinty, Verstraete, & Govaerts, 1999).
SeaWiFS (L3/L2) (WWW7)	Sep 1997–	1 month/daily	0.5°/1 km	Plate-carrée/sinusoidal	Polynomial formula based on 1D RT model (Gobron, Pinty, Verstraete, & Widlowski, 2000; Gobron et al., 2006).

2. Data and methods

The data used in this study include satellite and in-situ FAPAR measurements. Satellite products include MISR, MODIS, SeaWiFS, MERIS, and GEOV1 FAPAR products. The FAPAR validation data are collected from two groups of experimental sites: VAlidation of Land European Remote sensing Instruments (VALERI, WWW1) and AmeriFlux (WWW2). The VALERI sites are widely distributed around the world and useful for spatial validation over different land covers (Camacho et al., 2013; Weiss et al., 2007). Three years of measurements at AmeriFlux sites is intended for validating FAPAR products for a long period of time in consideration of their continuous measurements of FAPAR. The land covers of the 27 VALERI and AmeriFlux sites include 9 forests (1 of AmeriFlux and 8 of VALERI), 11 crops (3 of AmeriFlux and 8 of VALERI), 6 grass sites (of VALERI), and 1 shrubland site (of VALERI). Their distributions are shown in Fig. 1. The geolocation and land cover information of the AmeriFlux and the VALERI sites are listed in Table 1 for reference.

Four components are measured to compute FAPAR at AmeriFlux sites, including incoming and outgoing solar flux and flux from and to the ground. Incoming (outgoing) solar flux is measured with Li-Cor point quantum sensors aimed upward (downward), and placed at approximately 6 m above the ground. Flux transmitted through the

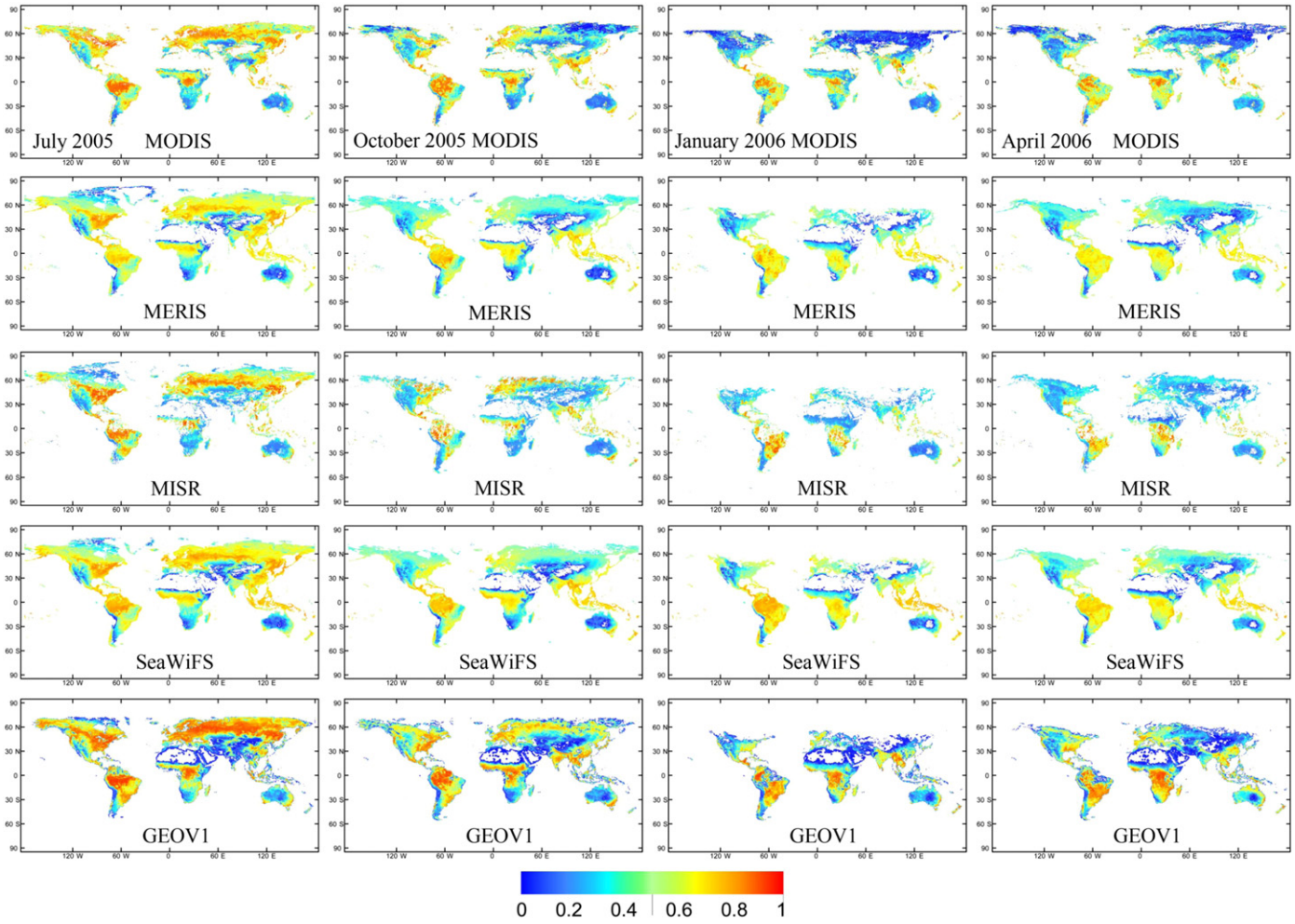

Fig. 2. The MODIS, MERIS, MISR, SeaWiFS, and GEOV1 global FAPAR distributions in Plate-carrée projection during the period July 2005–June 2006 (every 3 months). Note the agreements among the MODIS, MISR, and GEOV1 FAPAR products and between the MERIS and SeaWiFS FAPAR products. However, the MODIS, MISR, and GEOV1 FAPAR values were consistently higher than the MERIS and SeaWiFS FAPAR values.

canopy to the ground is measured with Li-Cor line quantum sensors placed at approximately 2 cm above the ground, pointing upward. Flux reflected by the ground is measured with Li-Cor line quantum sensors placed approximately 12 cm above the ground, pointing downward (Hanan et al., 2002). Hourly FAPAR is calculated as the ratio of absorbed photosynthetically active radiation and incoming solar flux. All the daytime radiation values are computed by integrating the hourly measurements during a day when incoming solar flux exceeded 1 μmol/m^2/s, and daily FAPAR is then calculated. Digital hemispherical photos are used to calculate FAPAR at VALERI sites, which corresponds to the fraction of intercepted PAR. High spatial resolution remote sensing data are used as a bridge to obtain the FAPAR values in the medium resolution pixels. The differences in the interception and the absorptions are small (less than 5%), which are taken into account by adding error bar on the in-situ data in this study considering the limited FAPAR ground-based data (Serbin et al., 2013).

Satellite FAPAR products have some differences in the definition of their products in terms of the whole canopy or green leaves, direct radiation only or not, and the imaging time. The MISR FAPAR product is the total FAPAR at 10:30 am, considering both direct and diffuse radiation absorbed by the whole canopy. The MODIS FAPAR considers only direct radiation, which may result in a smaller value than the MISR FAPAR product. The imaging time of the SeaWiFS sensor is approximately 12:05 pm local time, and its FAPAR product corresponds to the black sky FAPAR (direct radiation only) by green elements. Similarly, the MERIS FAPAR product corresponds to the black sky FAPAR by green elements at 10 am local time. The GEOV1 FAPAR product corresponds to the instantaneous black-sky FAPAR by green parts around 10:15 am local time. The SeaWiFS, MERIS, and GEOV1 FAPAR products take into account only the absorption by green elements, which may result in lower FAPAR values than the MISR and MODIS FAPAR products, which include the absorption of both green and non-green elements. Overall, most of the satellite FAPAR products correspond to the instantaneous black-sky FAPAR around 10:15 am which is a close approximation of the daily integrated FAPAR value collected at AmeriFlux and VALERI sites so that the validation of satellite FAPAR products using these ground-based measurements would be reasonable.

The spatial and temporal resolutions and the temporal coverage information of the satellite FAPAR products used in this paper, as well as their retrieval algorithms, are listed in Table 2. The spatial resolutions of the FAPAR products vary from 1 km to 0.5°, and the temporal resolutions vary from daily to 1 month. Spatial aggregation and temporal interpolation are necessary to intercompare the values across multiple scales. The MODIS and GEOV1 FAPAR products are preprocessed to be at the same temporal and spatial resolution than other products. The four 8-day MODIS FAPAR images are composited to monthly product from the average value of the highest quality data, in consideration of the quality of the output data and the small number of 8-day input data in a month. Average value is used because of the small number of 8-day valid observations in a month (maximum of 4). In consideration

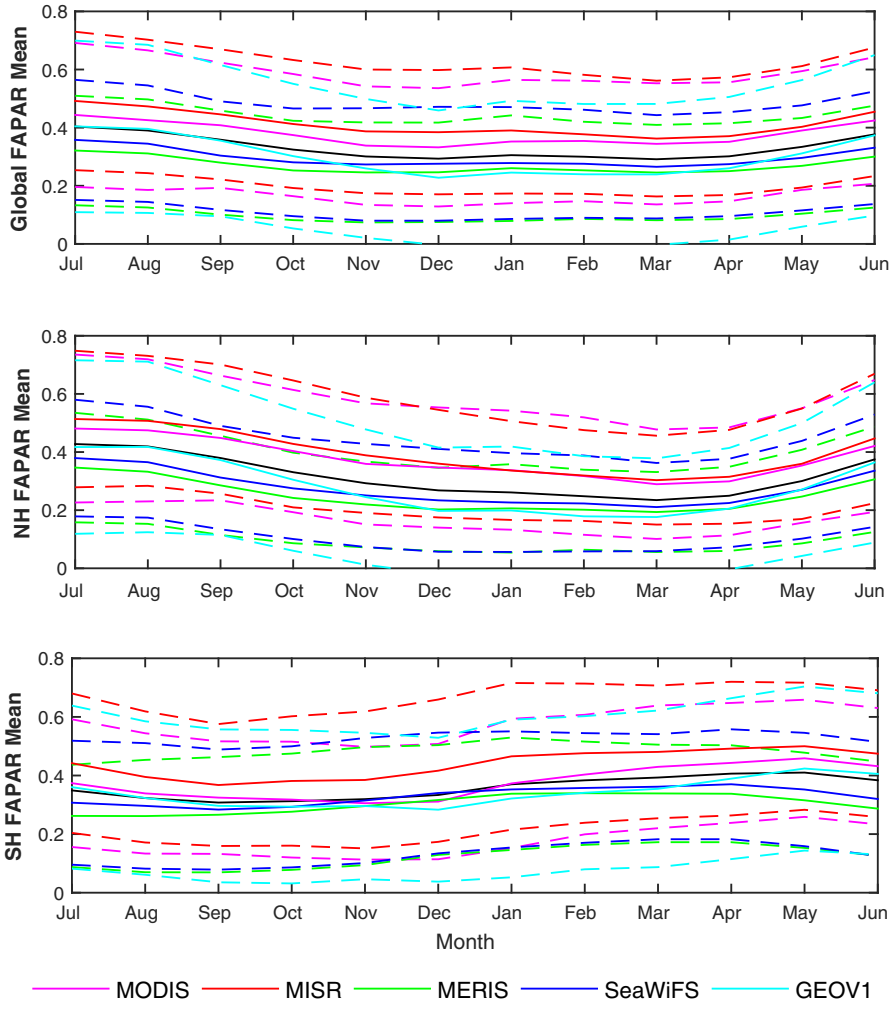

Fig. 3. The global, northern hemispheric, and southern hemispheric mean of quality controlled MODIS, MISR, MERIS, SeaWiFS, and GEOV1 FAPAR products during the period July 2005–June 2006. The black curve is all five products mean. The dashed curves correspond to the mean ± standard deviation of each product.

of the quality of the output, we generate the average value from the highest quality data in a month. The monthly 1 km product is resampled to 1/112° using nearest neighbor technique and then aggregated to 0.5° spatial resolution using spatial average. Similarly, the 30-day composite GEOV1 FAPAR product with the highest quality is spatially aggregated to 0.5° spatial resolution.

The different spatial scales between the FAPAR product pixels and the in-situ measurements can induce the scaling effect of FAPAR, which happens when the surface is heterogeneous and the retrieval algorithm is nonlinear (Tao et al., 2009; Xu, Fan, & Tao, 2009). Because of the scale difference, the validation results at more homogeneous sites are expected to have a higher FAPAR accuracy. We evaluate the heterogeneity around the validation sites by calculating the standard deviation divided by the mean of the simple ratio between near infrared and red bands of the Landsat data in the 1×1 km extent around the sites corresponding to the most common resolution of the satellite FAPAR products used for direct validation. The FAPAR accuracy at different sites is analyzed and the impact of site heterogeneity on the FAPAR product accuracy is explored.

3. Intercomparison of satellite FAPAR products

The MODIS, MERIS, MISR, SeaWiFS, and GEOV1 satellite FAPAR products are intercompared globally and over different land cover types in a one year period. Specifically, the spatial and seasonal distributions of the five satellite FAPAR products are intercompared globally in Section 3.1. The performances of the five satellite FAPAR products over different land cover types are intercompared in Section 3.2.

3.1. Intercomparisons over the globe

The spatial distribution of the five global FAPAR products during the period July 2005–June 2006 is depicted in Fig. 2. The MODIS global FAPAR product generally agrees well with the MISR and GEOV1 FAPAR product, while the MERIS and SeaWiFS FAPAR products agree well with each other. However, the difference between the group of MODIS, MISR, and GEOV1 FAPAR products and the group of MERIS and SeaWiFS FAPAR products is large (>0.1). The results are expected and the primary reason is that both the SeaWiFS and the MERIS FAPAR products correspond to absorbed fluxes for green leaf single scattering whereas the MODIS and MISR FAPAR products are based on a priori knowledge of leaf single scattering for each biome. The GEOV1 FAPAR correspond to a fused products which includes MODIS ones.

The seasonal distribution of the five preprocessed 0.5° spatial resolution FAPAR products over the entire globe and the Northern and Southern Hemispheres with the same number of pixels are depicted in the panels of Fig. 3. The MODIS FAPAR values remain relatively stable globally from December to March, then increase at an accelerating rate from April to July, and finally decrease from August to the lowest values in December. The trend in the Northern Hemisphere is slightly different, where FAPAR remains relatively stable from January (instead of December globally) to March, then increases from April to July, and finally decreases from August to January (instead of December globally, 1 month longer). The reason is an increase in vegetation FAPAR values from December in the Southern Hemisphere, so that global FAPAR would drop to the lowest value in December even if northern hemispheric FAPAR drops to the lowest value in January. The MERIS, MISR, SeaWiFS, and GEOV1 global FAPAR values have similar trends

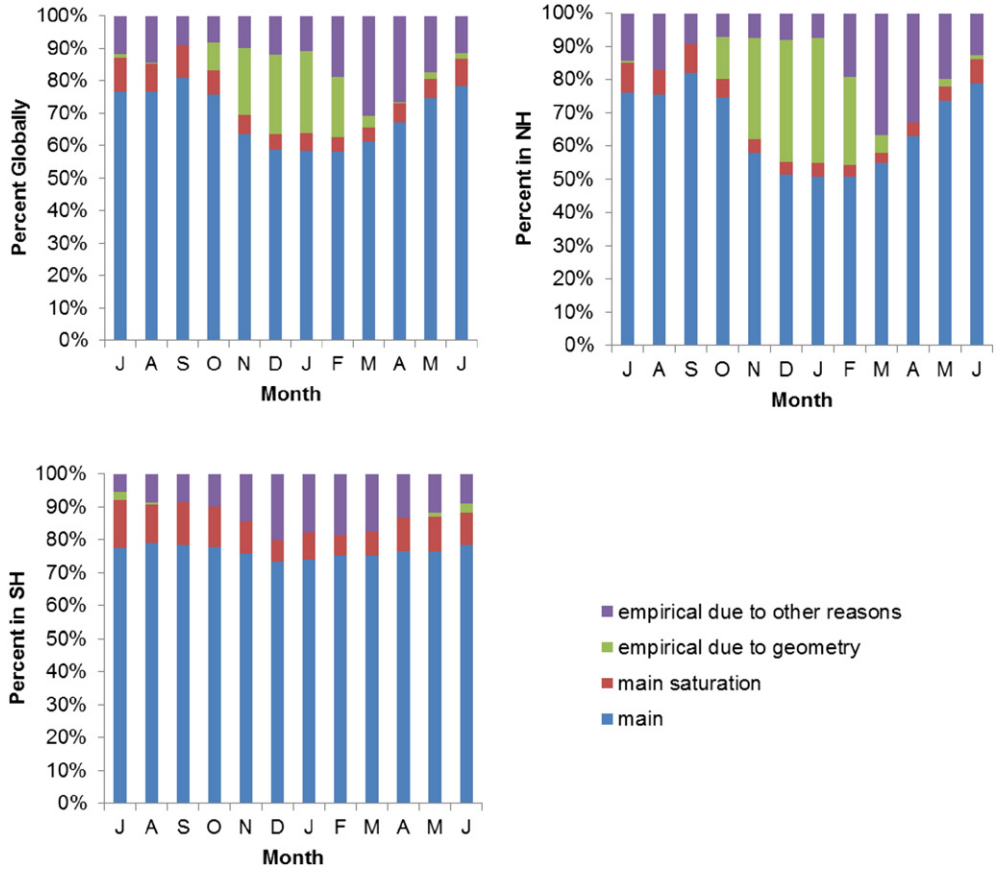

Fig. 4. MODIS collection 5 FAPAR QC statistics globally, in the Northern Hemisphere, and the Southern Hemisphere: the percentage of main algorithm retrievals (blue), the percentage of main algorithm under conditions of saturation (red), the percentage of backup (i.e. NDVI-based) retrievals associated with bad geometry (green), the percentage of pixels using the backup algorithm due to reasons other than geometry (purple). Note the overall increase in high quality (main algorithm) retrievals during the middle of the growing season.

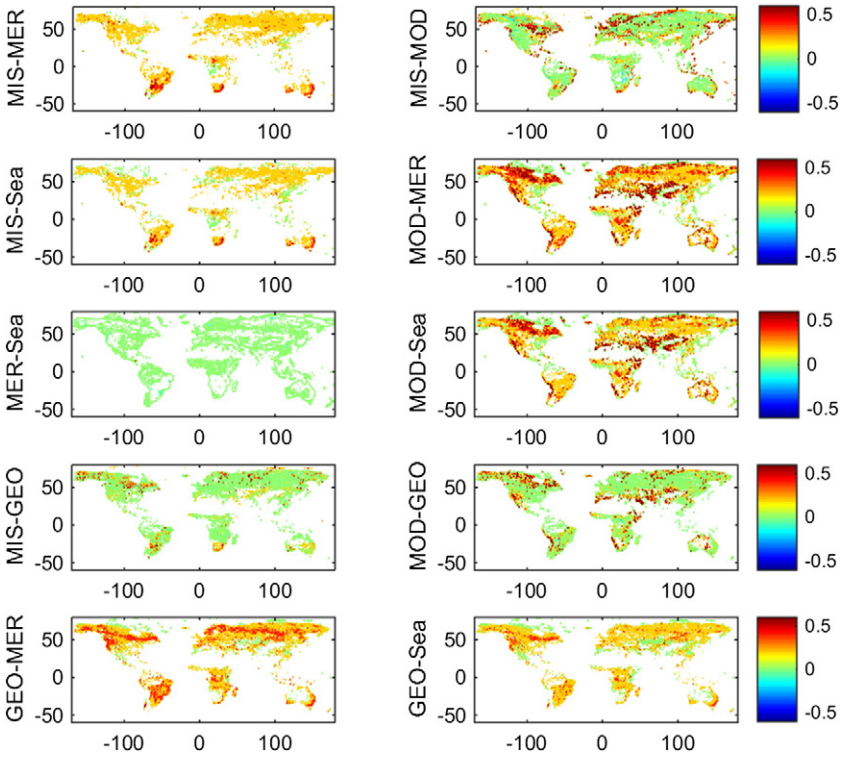

Fig. 5. Global FAPAR difference maps between the MODIS, MISR, GEOV1, MERIS and SeaWiFS products in July 2005 (MIS: MISR, MER: MERIS, MOD: MODIS, Sea: SeaWiFS, Geo: GEOV1).

as the MODIS global FAPAR values. Therefore, satellite FAPAR products agree well both globally and in the Northern Hemisphere in terms of trends. The differences of the mean values of the MODIS, MISR, and GEOV1 FAPAR products at the global scale are very small (<0.05 generally). The difference of the standard deviations of MODIS and MISR is less than 0.02. The mean values of the MERIS and SeaWiFS FAPAR products differ within 0.05 and the standard deviations differ within 0.015. However, the MODIS, MISR, and GEOV1 global FAPAR values are 0.05–0.1 higher than the average of the five products; whereas the MERIS and SeaWiFS global FAPAR values are 0.05–0.1 lower than the average in terms of magnitudes. Absolute FAPAR values are on average in decreasing order from MISR to MODIS to GEOV1 to SeaWiFS and MERIS (McCallum et al., 2010).

The difference between the MODIS, MISR, and GEOV1 FAPAR products become greater in other seasons than in the vegetation growing season, with the mean values differing by approximately 0.05. The differences between the mean of the MERIS and SeaWiFS FAPAR products remain stable and do not depend on the vegetation growing season. The difference between the group of MODIS, MISR, and GEOV1 FAPAR products and the group of MERIS and SeaWiFS FAPAR products becomes greater in other seasons (~0.16). The differences in the standard deviations between 2 months were within 0.02 for any of the five global FAPAR products. Therefore, the standard deviation of global FAPAR is almost independent of the month for these FAPAR products.

Compared with the FAPAR trends in the Northern Hemisphere, opposite situations are found in the FAPAR trends in the Southern Hemisphere. The MODIS and GEOV1 southern hemispheric FAPAR remain relatively stable from August to November, then increase to the highest values in May, and finally drop to the lowest values in November. The MISR southern hemispheric FAPAR has similar trend as the MODIS and GEOV1 southern hemispheric one, except that it drops to the lowest values near September instead of November. The MERIS southern hemispheric FAPAR is slightly different from the MODIS and MISR one. It remains relatively stable from July to September, then increases to the highest values in February, and finally drops to the lowest values near August (3 months variation from MODIS). The SeaWiFS southern hemispheric FAPAR remains relatively stable from July to September, then increases to the highest values in April, and finally drops to the lowest values in September (same as MISR). Overall, southern hemispheric FAPAR remains relatively stable from August to November,

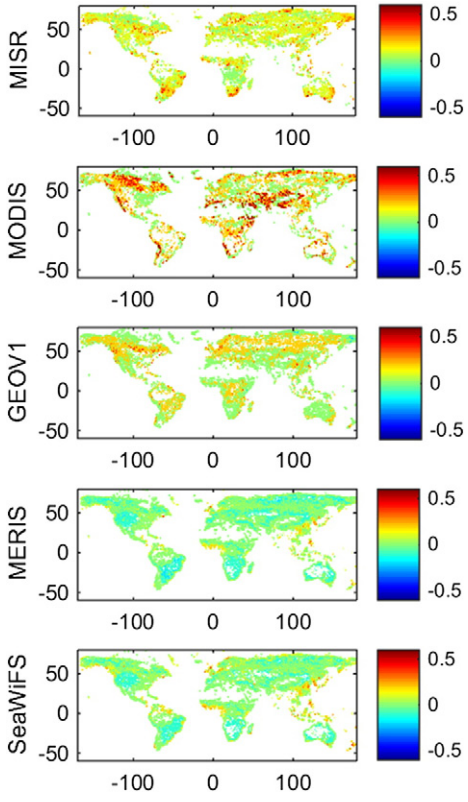

Fig. 6. Maps of the five global FAPAR datasets in July 2005, with the mean of all five products per grid-cell subtracted from each dataset.

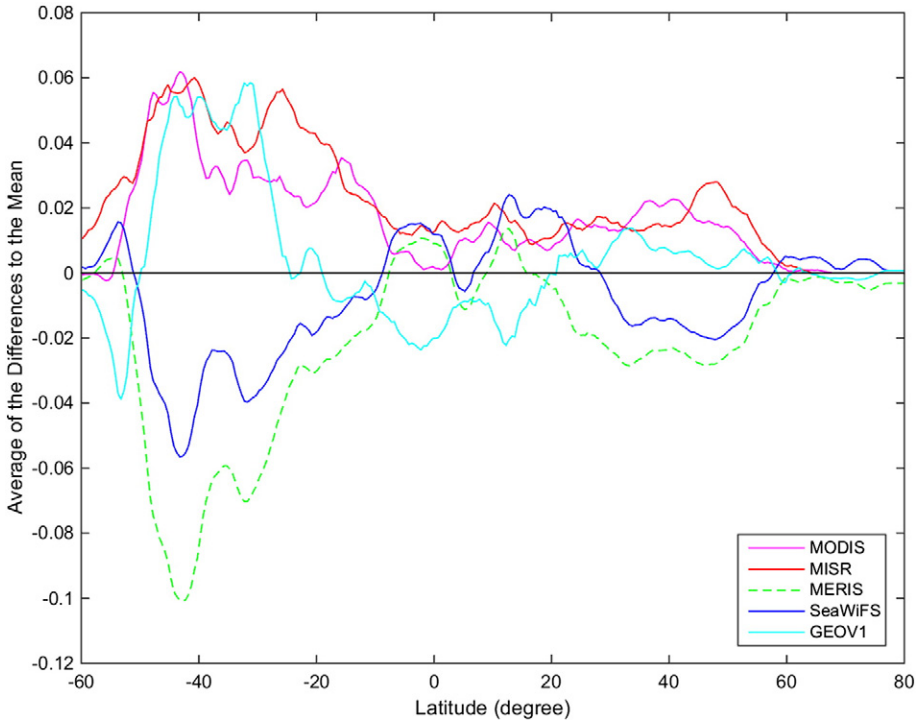

Fig. 7. The average of the difference to the mean of the five products at different latitudes in July 2005. The black line is for reference.

then increases to the highest values in April or May, and finally drops to the lowest values between September and November. The increased disparity among products in the Southern Hemisphere is likely a result of fewer vegetation samples there, which is explored in detail for different land covers in Section 3.2.

The quality flags of MODIS FAPAR data are analyzed to select maps in high quality month for further comparisons. The statistics of MODIS Collection 5 FAPAR quality control flags are depicted globally and in the Northern and Southern Hemispheres (Fig. 4). The percentage of the main algorithm retrievals increases in the middle of the growing season and reaches the highest value in September. The percentage of backup retrievals due to bad geometry increases in the winter as expected because of the larger solar zenith angle. This kind of backup retrieval related to bad geometry lasts 6 months, from October to March, both globally and in the Northern Hemisphere and approximately 3 months, from May to July, in the Southern Hemisphere. Overall, the analysis on the MODIS quality flags shows that the quality of satellite FAPAR products is better in the vegetation growing season than other season.

The difference maps between satellite FAPAR products in July are depicted in Fig. 5. The sea/land mask is applied and only pixels with high quality values from all of the five satellite FAPAR products are included in the difference maps. The MISR FAPAR product exhibits some higher FAPAR values than the MERIS and SeaWiFS FAPAR products at high latitudes, and some slightly lower FAPAR values in the tropical forests near the equator. The difference between the MERIS and SeaWiFS FAPAR products is very small, with a few pixels located along the boundaries of continents. The difference between the MISR and MODIS FAPAR products is quite small as well, with only a few scatters in the boreal forests of Asia and North America. The MISR and MODIS FAPAR products are close to the GEOV1 FAPAR product, except some

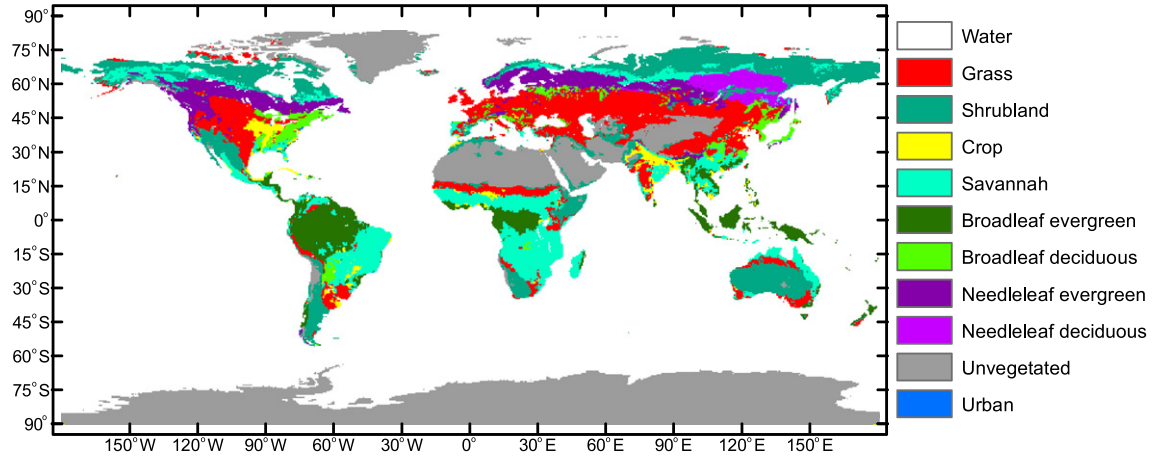

Fig. 8. The resampled MODIS global land cover map (MCD12) at 0.5° during the period July 2005–June 2006. The vegetated areas are classified by use of the MODIS-derived LAI/FAPAR scheme into eight land cover types: broadleaf evergreen forest, broadleaf deciduous forest, needleleaf evergreen forest, needleleaf deciduous forest, crop, grass, savannah and shrubland. The map also includes the unvegetated, water, and urban area.

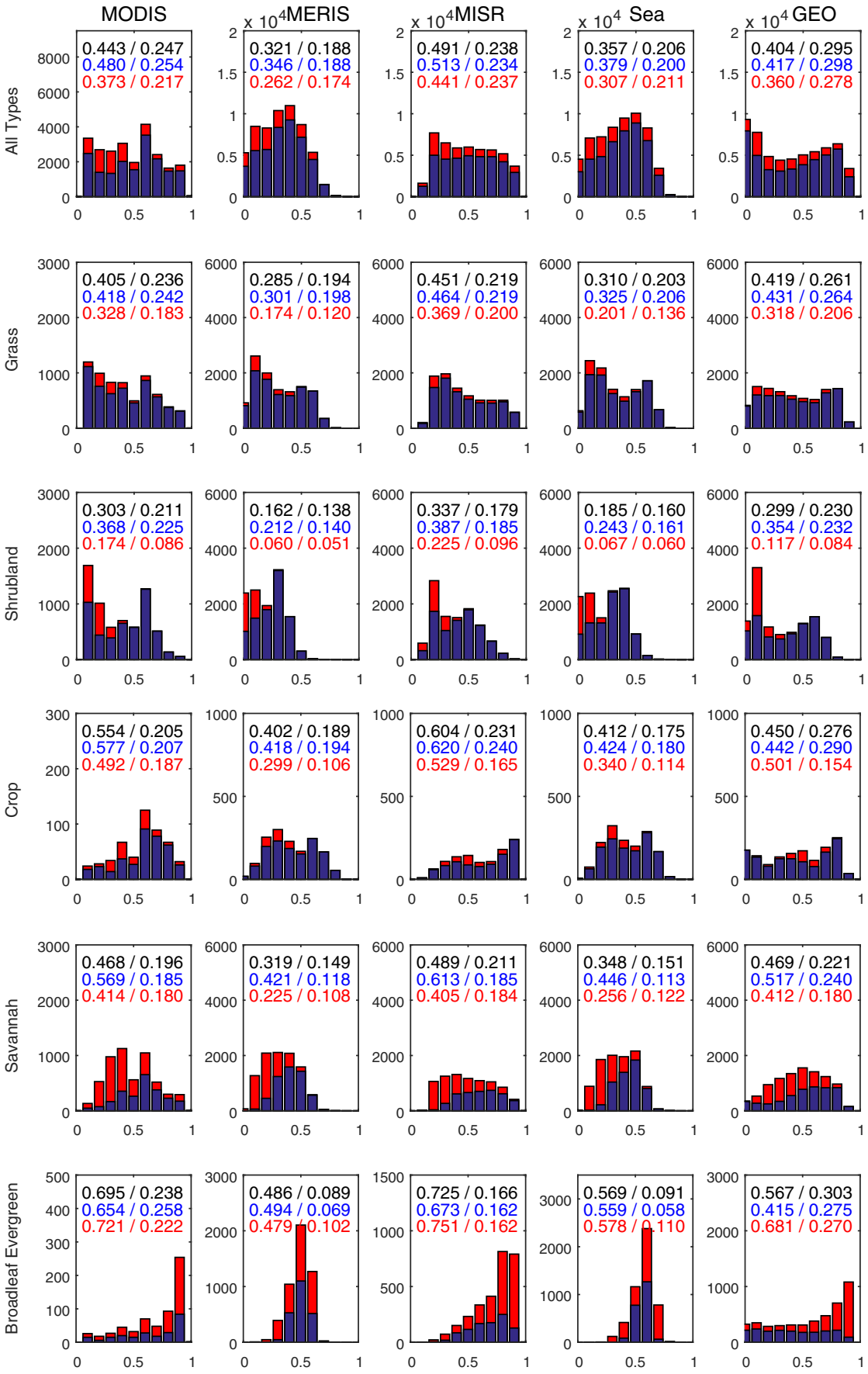

Fig. 9. Histograms of the quality controlled MODIS, the MERIS, the MISR, the SeaWiFS, and the GEOV1 FAPAR products over all or individual land cover types in the entire globe (black), the Northern Hemisphere (blue), and the Southern Hemisphere (red) in July 2005. The numbers are the mean and the standard deviations of FAPAR over the entire globe (black), the Northern Hemisphere (blue), and the Southern Hemisphere (red).

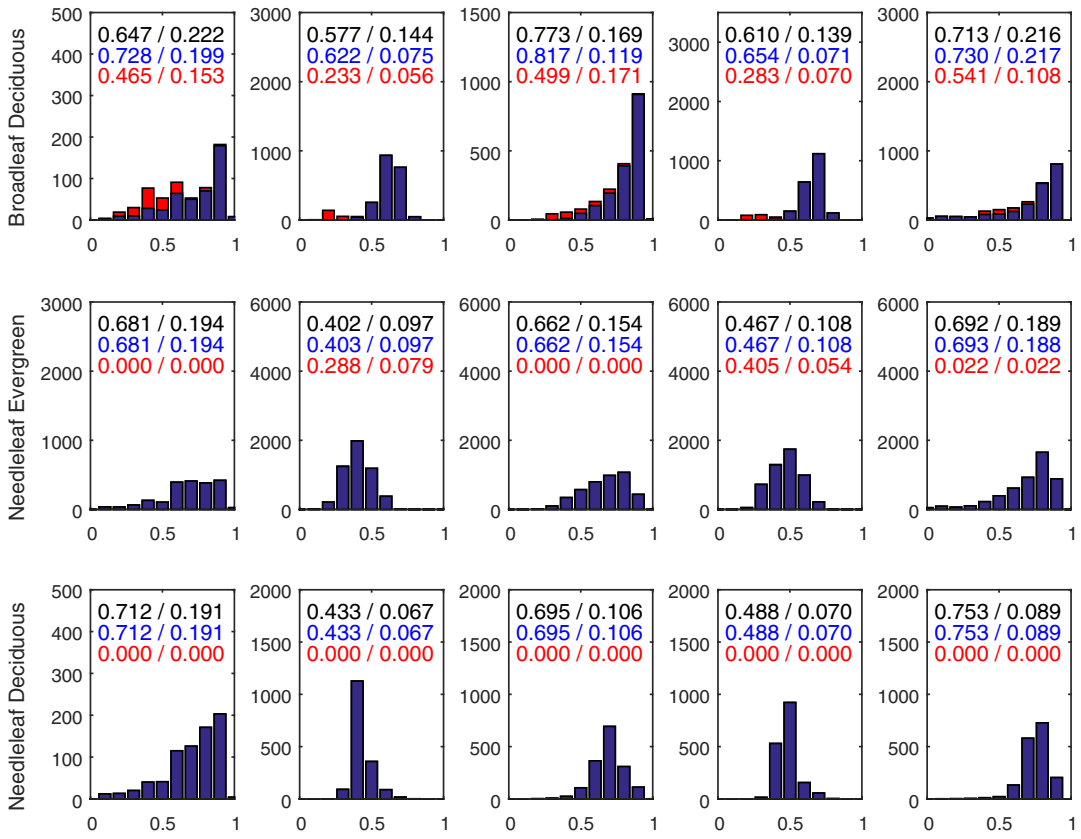

Fig. 9 (*continued*).

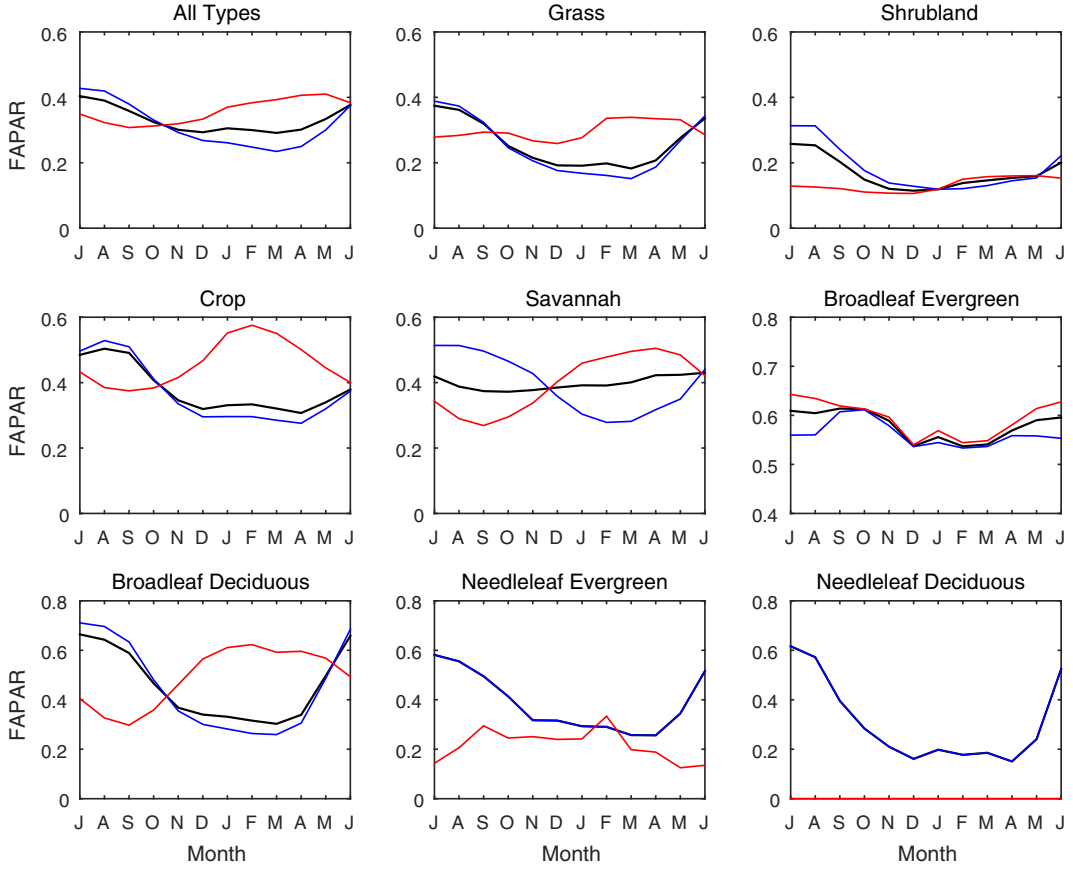

Fig. 10. The global (black), northern hemispheric (blue), and southern hemispheric (red) FAPAR mean of all five products over different land cover types during the period July 2005–June 2006.

boundary regions. However, the MODIS FAPAR values are apparently higher than the MERIS and SeaWiFS FAPAR values over the boreal forests and savannahs. The GEOV1 FAPAR product is consistently higher than the MERIS and SeaWiFS FAPAR products over the tropical and boreal forests.

The five global FAPAR datasets are averaged per grid cell and then subtracted from each dataset to obtain the difference to the mean maps (Fig. 6). The MODIS, MISR, and GEOV1 FAPAR products have larger values than the average in the boreal and tropical forests and grasslands in the Northern Hemisphere. The GEOV1 FAPAR products are closest to the average of all the products. The MERIS and SeaWiFS FAPAR products have apparently lower than the average values in the forests, savannahs and grasslands. The differences to the mean maps are averaged across different latitudes (Fig. 7). Their differences are smaller at low and high latitudes but are larger at middle latitudes, especially in the Southern Hemisphere. The possible reason is the saturation of FAPAR values in the tropical forests and the scarcity of vegetation in the high latitudes so that the differences are smaller in these regions.

3.2. Intercomparisons over different land cover types

The MODIS global land cover map (MCD12) during the period July 2005–June 2006 is depicted in Fig. 8. The vegetated areas are classified by use of the MODIS-derived LAI/FAPAR scheme into eight land cover types: broadleaf evergreen forest, broadleaf deciduous forest, needleleaf evergreen forest, needleleaf deciduous forest, crop, grass, savannah, and shrubland (Myneni et al., 2002). The MCD12 land cover classification product was resampled into 0.5° using the mode resampling method by selecting the value which appears most often of all the sampled points. Most of the vegetated areas are located in the Northern Hemisphere. The only exception is the broadleaf evergreen forests, the majority of which are located in the Southern Hemisphere, including the northwest part of South America, part of Central Africa, and the southern part of Southeast Asia.

The histograms of the MODIS, MERIS, MISR, SeaWiFS, and GEOV1 FAPAR products over different land cover types are depicted in Fig. 9, where the blue bars denote the number of pixels in the Northern Hemisphere, and the red bars denote the number of pixels in the Southern Hemisphere. The MODIS, the MISR, and the GEOV1 FAPAR agree well with each other over different land cover types, and so do the MERIS and the SeaWiFS FAPAR. The MODIS, MISR, and GEOV1 FAPAR are consistently higher than the MERIS and SeaWiFS FAPAR because the former ones detect much more pixels with FAPAR values over 0.8 than the latter, especially over tropical forests. The differences in the magnitudes could be attributed to the different composite algorithms. Both global MERIS and SeaWiFS monthly products correspond to median values in a month instead of average values as the MODIS, MISR, and GEOV1 FAPAR products. In such case, there are fewer high FAPAR values in the MERIS and SeaWiFS FAPAR products than in other products. Absolute FAPAR values are on average in decreasing order from MISR to MODIS to GEOV1 to SeaWiFS and MERIS over almost all land cover types except needleleaf forests. The MODIS FAPAR is higher than the MISR FAPAR over needleleaf forests, because more pixels with high FAPAR values are detected over needleleaf forests in the MODIS FAPAR product than in the MISR FAPAR product. The GEOV1 FAPAR product is very close to the MODIS FAPAR product, with slight deviations over broadleaf evergreen forests. Regarding the differences of the mean of the products over the Northern and Southern Hemispheres, the mean FAPAR is higher in the Northern Hemisphere than in the Southern Hemisphere over most of the land cover types except broadleaf

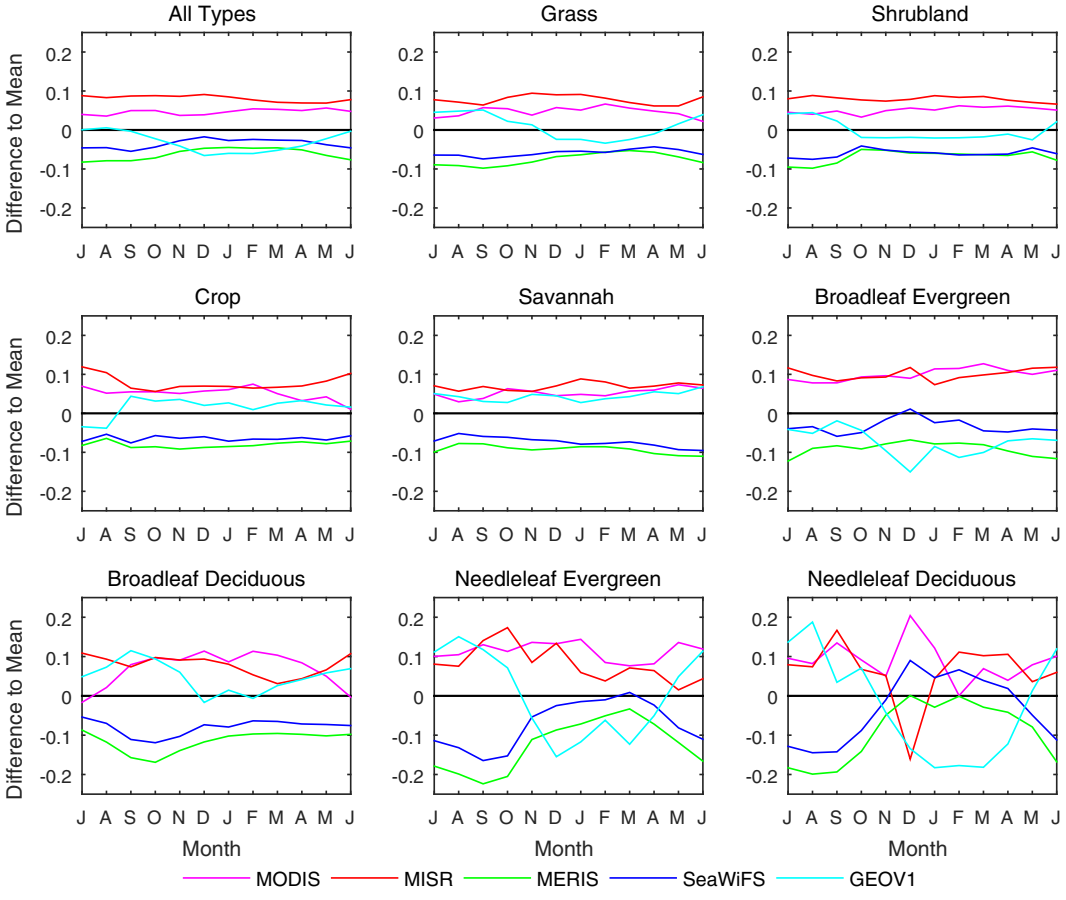

Fig. 11. The time series of the mean of quality controlled MODIS, MISR, MERIS, SeaWiFS, and GEOV1 FAPAR products over different land cover types during the period July 2005–June 2006, with the mean of all five products subtracted from each dataset. The black line is for reference.

evergreen forest for the five products during the northern hemispheric vegetation growing season. The mean FAPAR over broadleaf evergreen forest in the Southern Hemisphere is slightly higher (~0.02) than in the Northern Hemisphere. The mean of all five products is averaged globally and in the Northern and Southern Hemispheres during the period July 2005–June 2006 to show their seasonal patterns at the three scales (Fig. 10). The southern hemispheric FAPAR is constantly higher than the northern hemispheric FAPAR over broadleaf evergreen forests, regardless of season.

The trend of northern hemispheric FAPAR is similar to that of global FAPAR, with slight difference in the magnitudes (Fig. 10). The explanation is that the majority of the land cover is located in the Northern Hemisphere, resulting in the dominant influence of northern hemispheric FAPAR on global FAPAR. The exceptions are the FAPAR over savannah and broadleaf evergreen forest land covers. The global FAPAR mean over savannah remains almost constant throughout the year, but the northern hemispheric FAPAR mean is a sine curve, with the highest value in September and the lowest value between February and March. There is an opposite trend in the Southern Hemisphere, and the two trends cancel each other out globally. The global FAPAR mean over broadleaf evergreen forest is stabilized throughout the year, but the northern hemispheric FAPAR is a sine curve. In this case, the curve of the global

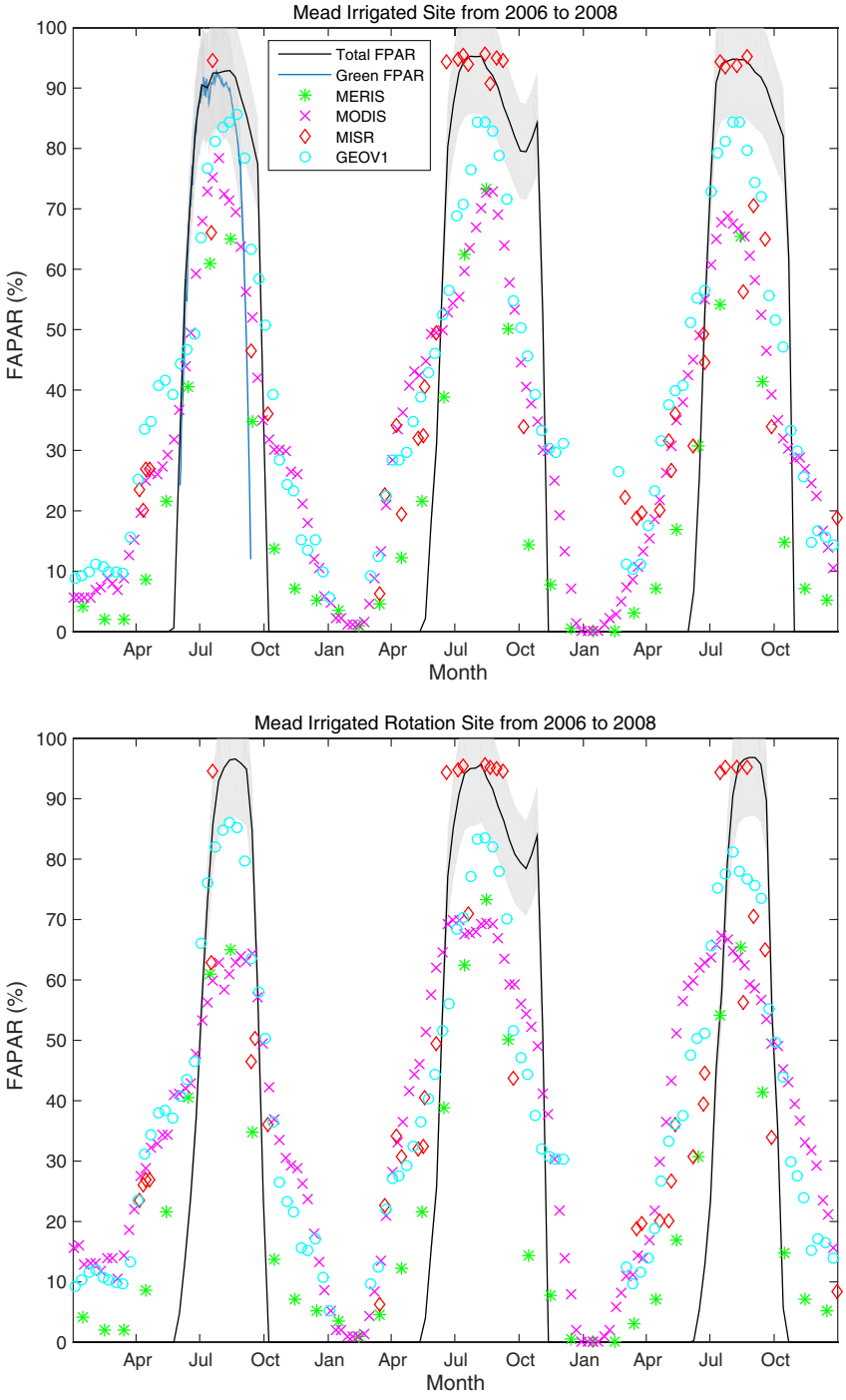

Fig. 12. The time series of in-situ FAPAR measurements and satellite products at four AmeriFlux sites. Green FAPAR measurements are depicted in blue line in the first panel, and total FAPAR measurements are depicted in black line in all panels. The shaded area is the 10% accuracy requirement. The monthly MERIS, 8-day MODIS, 2–9 day MISR, and 10-day GEOV1 FAPAR products are depicted in asterisks, crosses, diamonds, and circles, respectively.

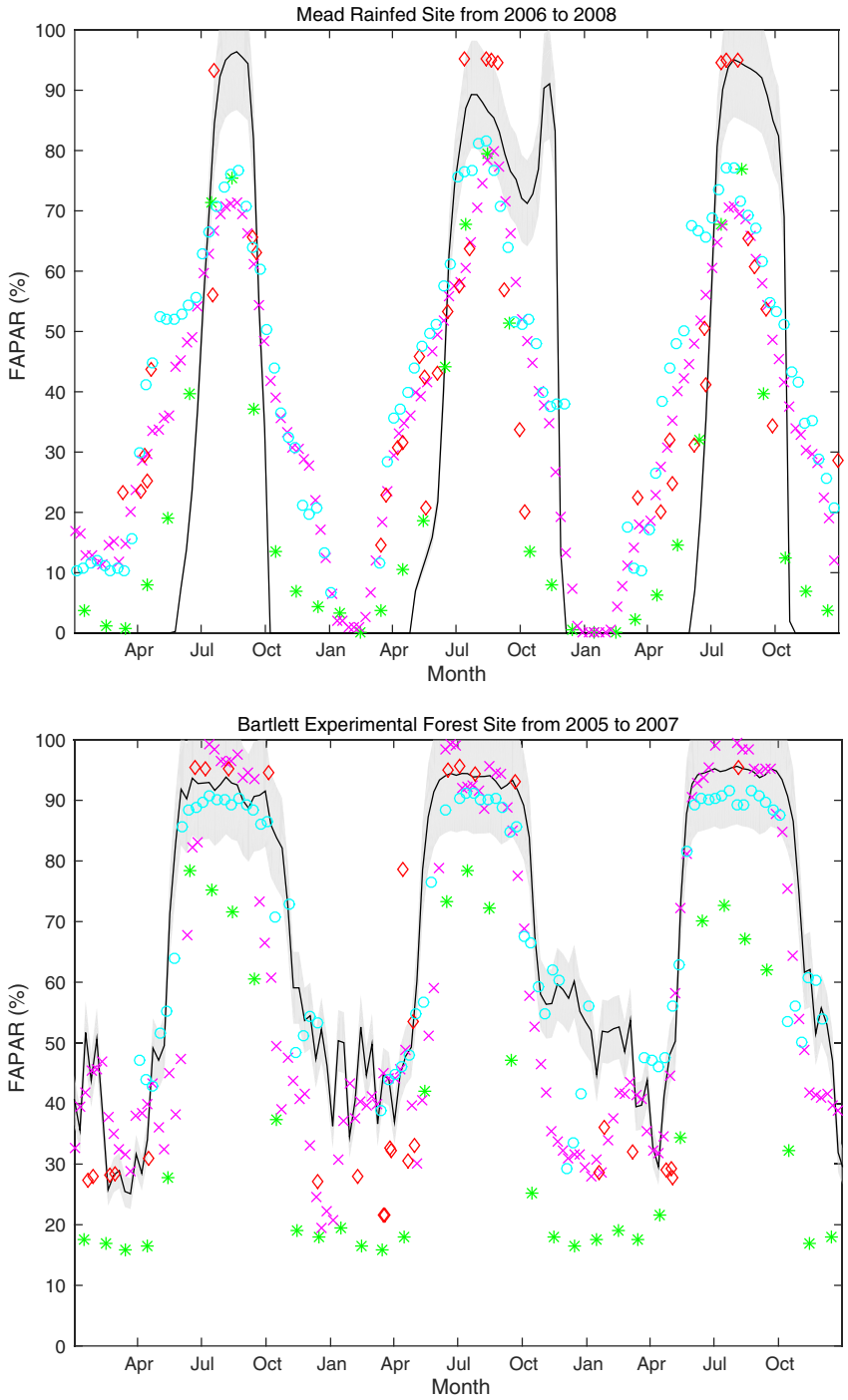

Fig. 12 (*continued*).

FAPAR mean is similar to the curve in the Southern Hemisphere, because the majority of broadleaf evergreen forests are located in the Southern Hemisphere as noted.

Compared with the trends of the northern hemispheric FAPAR mean, opposite trends are found in the southern hemispheric FAPAR mean. The opposite relations are very apparent globally, over crop, savannah, grass, broadleaf deciduous forest, and needleleaf evergreen forest. The opposite relations are not apparent over shrubland and broadleaf evergreen forest, where the southern hemispheric FAPAR is stabilized throughout the year, but the northern hemispheric FAPAR mean has a parabolic shape over shrubland and a sine curve over broadleaf evergreen forest. The global FAPAR curve overlaps with the northern hemispheric FAPAR curve over needleleaf evergreen forests, provided that only a few needleleaf evergreen forests are in the Southern Hemisphere. Barely any needleleaf deciduous forests are in the Southern Hemisphere. Both the northern hemispheric and the global FAPAR mean have bowl-like shapes over needleleaf deciduous forests throughout the year.

The time series of the mean of the MISR, MODIS, GEOV1, SeaWiFS, and MERIS FAPAR products over different land cover types during the period July 2005–June 2006 are depicted in Fig. 11, with the mean of all five products subtracted from each dataset. The MODIS and MISR FAPAR products are approximately 0.05–0.1 higher than the average of the five products, and the MERIS and SeaWiFS FAPAR products are

Table 3
Statistics of comparisons between ground-based and space products.

Site	Product	RMSE	Bias	R^2
Mead Irrigated	MERIS	0.182	−0.092	0.777
	MODIS	0.145	0.009	0.667
	MISR	0.142	0.072	0.761
	GEOV1	0.114	0.067	0.773
Mead Irrigated Rotation	MERIS	0.161	−0.036	0.751
	MODIS	0.159	0.098	0.546
	MISR	0.124	0.104	0.733
	GEOV1	0.113	0.106	0.752
Mead Rainfed	MERIS	0.186	−0.060	0.668
	MODIS	0.143	0.070	0.626
	MISR	0.125	0.043	0.638
	GEOV1	0.149	0.113	0.577
Bartlett	MERIS	0.127	−0.290	0.749
	MODIS	0.167	−0.085	0.642
	MISR	0.103	−0.086	0.842
	GEOV1	0.075	−0.039	0.800

approximately 0.05–0.1 lower than the average of the five products. The GEOV1 FAPAR product has very small difference (<0.05) to the mean over grass, shrubland, crop and savannah. The deviations to the mean for the five products remain stable over grass, shrubland, crops, savannah, and broadleaf evergreen forests throughout the year. However, a different situation occurs over broadleaf deciduous forests, where the deviations are largest in October and smallest in June and July. The deviations of the five products from the average over needleleaf evergreen and needleleaf deciduous forests are largest in September and October, and gradually decrease to the lowest values in March. The GEOV1 FAPAR product has large fluctuations over needleleaf evergreen and needleleaf deciduous forests because of its strong seasonal pattern over the needleleaf forests with a standard deviation of 0.21, compared with standard deviations around 0.11 for other FAPAR products. In such case, it fluctuates both above and below the average line, although it has similar seasonality as other products as shown in Fig. 3. The MISR FAPAR product has a drop in the value over needleleaf deciduous forest in December because of no data. Overall, the differences between the products are consistent throughout the year over most of the land cover types, except over the forests. The possible reason can be traced to the different assumptions in the retrieval algorithms over forests and the large differences between green and total FAPAR products due to tree trunks and branches absorption (Pickett-Heaps et al., 2014). Interestingly, the differences between the products do not fluctuate much in broadleaf evergreen forests over time, because FAPAR values remain relatively stable all year long and therefore the differences between the products are small and consistent over broadleaf evergreen forests.

4. Direct validation of satellite FAPAR products

Satellite FAPAR products at 1 km are used for direct validation against 3 years of ground-based continuous measurements of FAPAR at 4 AmeriFlux sites. The validation results of the MERIS, MODIS, MISR, and GEOV1 FAPAR products with in-situ measurements at the AmeriFlux sites are shown in Fig. 12. The curves of the SeaWiFS FAPAR product are similar to those of the MERIS FAPAR product, so not shown here for clarity. The MISR FAPAR values are higher than the MODIS, MERIS, and GEOV1 FAPAR values, especially in the middle of the vegetation growing season. The in-situ FAPAR proxy at Mead Irrigated, Mead Irrigated Rotation, and Mead Rainfed sites reach zero before early April and after middle November, which is the result of harvesting the crops there. Most satellite FAPAR product values around the two sites approach, but are not exactly, zero at the beginning and end of

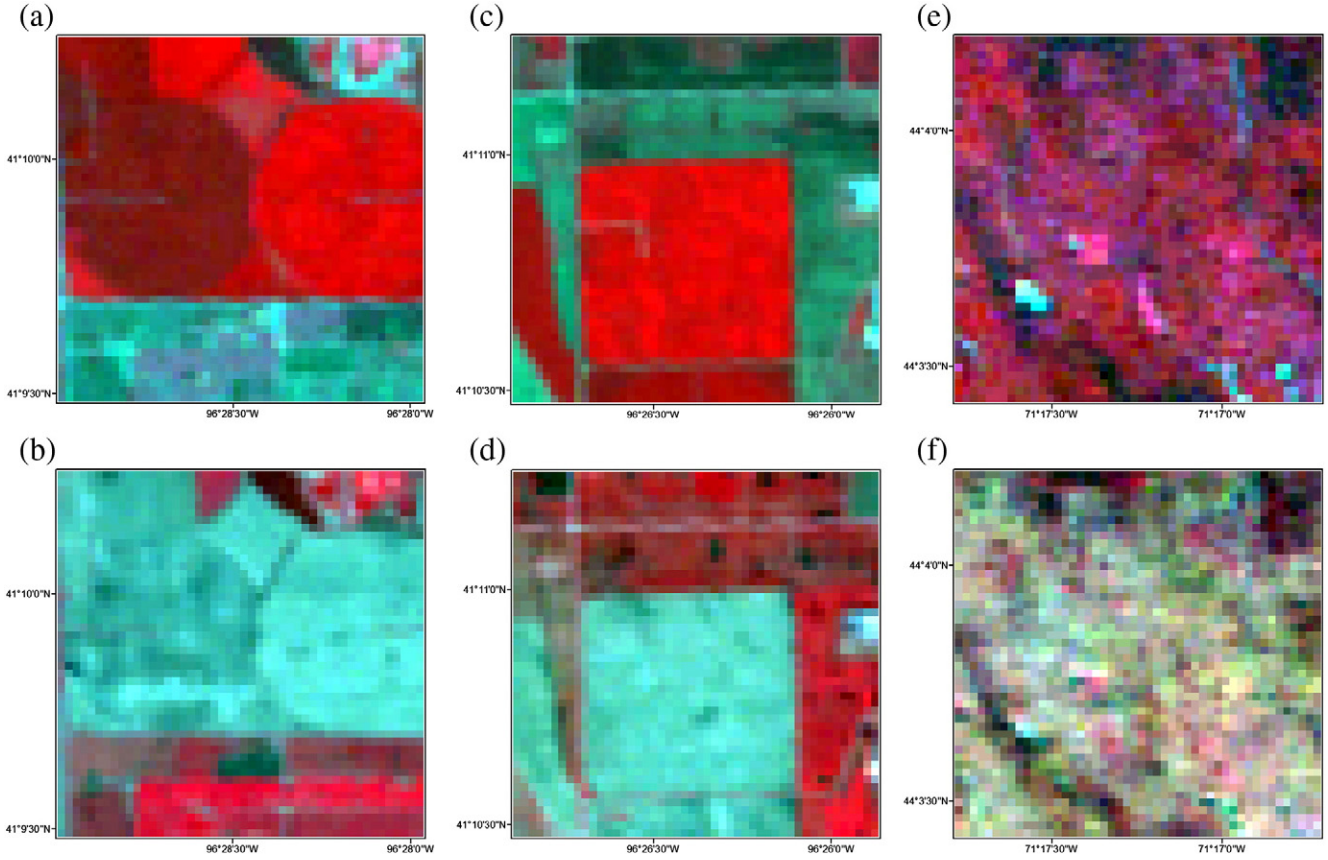

Fig. 13. Landsat images with an extent of 1440 m by 1440 m around Mead Irrigated and Mead Irrigated Rotation sites (a and b), Mead Rainfed site (c and d), and Bartlett site (e and f) during the vegetation growing season (a, c, e) and other seasons (b, d, f).

the year, which is caused by the contribution from inhomogeneous land cover, in addition to crops near the sites, or the limited soil reflectance database used by the algorithm (Tao et al., in review). The statistics of comparisons between ground-based and satellite FAPAR products are listed in Table 3. The MISR FAPAR product has the highest accuracy over the Mead Rainfed crop site. The GEOV1 FAPAR product has the best accuracy over other crop and forest sites. The MODIS, MISR, and GEOV1 FAPAR products agree better with in-situ measurements at the Bartlett experimental deciduous broadleaf forest site in magnitude than the MERIS FAPAR product does. The MERIS product has a good seasonality profile and little variation of random error caused by cloud contamination, but underestimates FAPAR by 0.12 overall. The underestimation is caused by the green leaf FAPAR estimated by MERIS versus the total FAPAR by ground-based measurements which include the absorptions of both leaf and non-leaf elements.

The validation results are improved when green FAPAR measurements are used as reference data, shown as a magenta line for the year 2006 in the first panel of Fig. 12. The improvement is significant for green FAPAR products, with the root mean square error (RMSE) reduced from an average of 0.15 to 0.08. Therefore, the accuracy of satellite green FAPAR products is improved when validated using green FAPAR instead of total FAPAR measurements. The main reason is the senescence and yellow turning of the leaves at the end of the growing season, and the green FAPAR, estimated by a multispectral optical remote sensing approach, would naturally agree better with in-situ measured green FAPAR than a higher value of total FAPAR (Vina & Gitelson, 2005; Zhang et al., 2005). However, the RMSE error for the MISR total FAPAR product is increased from 0.14 to 0.15. This is understandable as the MISR FAPAR product is total FAPAR and would naturally agree better with total FAPAR measurements. The MODIS FAPAR product has a slightly increased accuracy validated with green FAPAR measurements because of its inclusion of direct radiation absorption only, which has an offset from the ground-based FAPAR including both direct and diffuse radiation. Overall, the RMSE of all FAPAR products have been reduced from an average of 0.14 to 0.09. However, the calculation of green FAPAR requires additional simultaneous measurements of green LAI and total LAI to distinguish between green leaves and yellow leaves. The process is labor extensive, and thus green FAPAR measurements are not collected for all the years. Therefore, total FAPAR measurements are used as the main validation data in this study, considering its temporal continuity.

We evaluated the site homogeneity during the vegetation growing season and other seasons using Landsat images at 30 m high resolution. The satellite images within an extent of 1440 m by 1440 m around the sites are depicted in Fig. 13. We calculated the standard deviation divided by the mean of the simple ratio between near infrared and red bands in the three regions (the first region contains two sites: Mead Irrigated and Mead Irrigated Rotation). The values for the Mead Irrigated region are 0.586 and 0.573 during the vegetation growing season and other seasons, respectively. The values for the Mead Rainfed region are 0.747 and 0.381, and the values for the Barlett region are 0.162 and 0.147, respectively. With a smaller ratio between the standard deviation and the mean of the simple ratio, the vegetation in the Barlett region is more homogeneous than in the two Mead regions, and therefore FAPAR is expected to have higher validation accuracy and lower RMSE than that in the other two regions (Table 3). The averages of the homogeneity index of the two Mead regions are very close, but the homogeneity index of the Mead Irrigated region remains relatively stable. Therefore, higher validation accuracy is expected in the Mead Irrigated region than in the Mead Rainfed region.

The MODIS, MERIS, MISR, and GEOV1 FAPAR products are compared with the ground-based measurements at the VALERI experimental sites, as shown in Fig. 14. Generally speaking, the MERIS, SeaWiFS, and GEOV1 FAPAR have higher accuracy than the MODIS and MISR FAPAR regarding R^2 and RMSE at these sites. There are missing or invalid MERIS FAPAR values at five sites, GEOV1 FAPAR values at four sites, and MISR FAPAR values at three sites; thus, the retrieval rates of the MERIS, GEOV1, and MISR FAPAR products are lower than that of the MODIS and SeaWiFS FAPAR products. The MERIS, SeaWiFS, and GEOV1 FAPAR products perform well at all of the four land cover types, although the MERIS

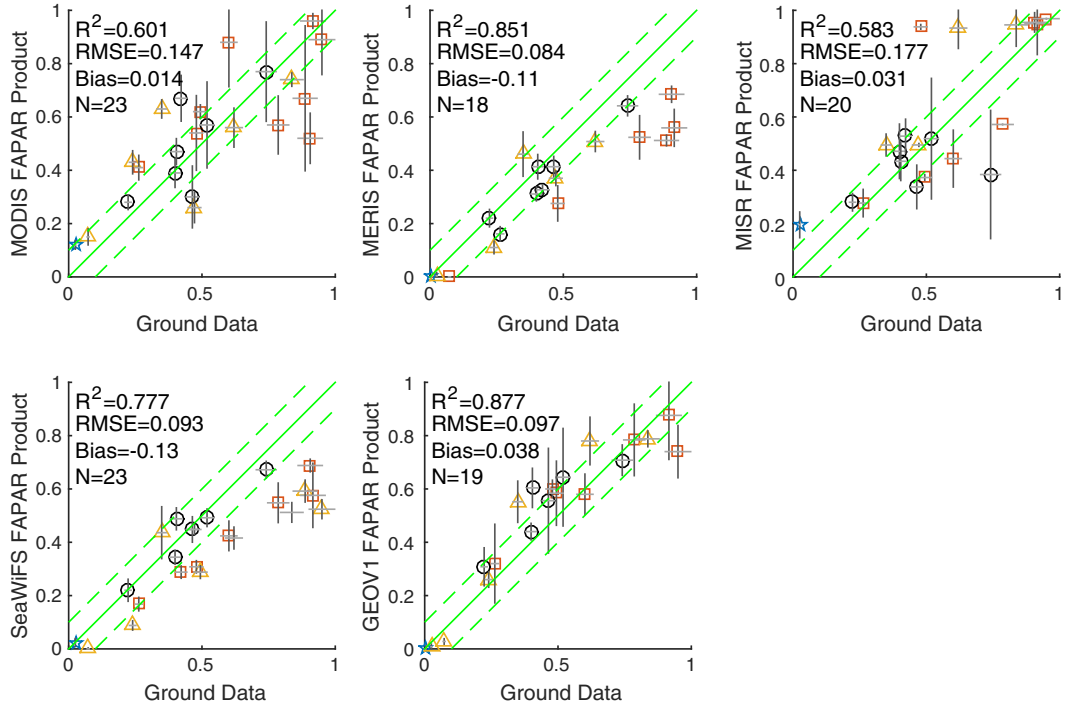

Fig. 14. The MODIS, MERIS, MISR, SeaWiFS, and GEOV1 FAPAR products validated with in-situ measurements of VALERI. The land cover of shrubland is represented by a pentagram (⋆), grass by triangle (△), forest by square (□), and crops by circle (○). Horizontal and vertical bars correspond to the uncertainties (±σ). The middle green line is y = x. The two other green lines are y = x ± 0.1, respectively.

and SeaWiFS FAPAR products slightly underestimate FAPAR compared with in-situ measurements. The MODIS FAPAR product performs well at crop sites. The MISR FAPAR product has better performance than the MODIS FAPAR product at grass and forest sites. The MODIS and MISR FAPAR products do not rank high in terms of R^2 and RMSE, but have satisfactory biases close to zero values.

5. Discussion

The intercomparison studies on the five satellite FAPAR products revealed some discrepancy among them. The FAPAR products have some general relations, in which the MISR FAPAR product often has the highest value, followed by the MODIS, GEOV1, and SeaWiFS FAPAR products, and the MERIS FAPAR product provides the lowest value. The difference could be partly explained by the differences in the definitions of FAPAR among products. The SeaWiFS, MERIS, and GEOV1 FAPAR products take into account only the absorption by green elements, resulting in lower FAPAR values than the MISR and MODIS FAPAR products, which include the absorption of both green and non-green elements. The difference between the SeaWiFS and MERIS FAPAR products is small, and it can be attributed to the differences in the satellite overpass time and cloud masks (Gobron et al., 2008).

The intercomparison results of global FAPAR products over different land covers show that no noticeable global trend over savannah is observed, which is caused by the canceling trends of the northern and southern hemispheric FAPAR. Therefore, the difference in the trends of the global FAPAR products over savannah is not significant and is likely to be caused by some random error because of the small magnitude of the trends. The Amazon broadleaf evergreen forests exhibit slightly different seasonal patterns in the Northern Hemisphere from that in the Southern Hemisphere, but the seasonality is weak compared with that over other land cove types. There is a debate on whether a seasonal pattern exists in the Amazon forests. Myneni et al. (2007) have observed a seasonal pattern in the southern hemispheric Amazon rainforest from MODIS data. However, Morton et al. (2014) find consistent canopy structure and greenness during the dry season in the Amazon forests using observations from LiDAR and MODIS (its bidirectional reflectance effect is further corrected). As shown in this study, there could be a weak seasonal pattern over broadleaf evergreen forests in the Southern Hemisphere. The different findings in the two studies might be explained by the weak seasonal pattern and the large random error caused by the saturation problem of optical remote sensing over heavily leaved Amazon forests.

Regarding the performance of individual FAPAR products, the MERIS has high accuracy and a good seasonality profile, but might underestimate the FAPAR values by 0.05–0.15. Some other studies also find that the MERIS FAPAR product has an uncertainty or negative bias of 0.1(Pickett-Heaps et al., 2014). Martinez et al. (2013) calculate their FAPAR based on the MERIS MGVI algorithm, which turns out to be very low compared with hemispherical pictures based ground measurements, especially in some cultivated sites with bias around 0.16. Because the MERIS and SeaWiFS FAPAR products are very close to each other based on the difference map of the two products in Fig. 5 in Section 3, similar problems would exist in the SeaWiFS FAPAR product as well. Camacho et al. (2013) evaluate the performance of SeaWiFS FAPAR products at some VALERI sites, and find the bias of SeaWiFS to be 0.16 and RMSE to be 0.23, even higher than MERIS FAPAR product. The negative bias of the MERIS and SeaWiFS FAPAR products could be a result of their retrieval of green FAPAR value. Therefore, this study show that the accuracy of the MERIS and SeaWiFS FAPAR products could be significantly improved from 0.15 to 0.08 when validating with in-situ green FAPAR instead of total FAPAR measurements.

The general performances of the MODIS, MISR, and GEOV1 FAPAR products are good when compared with in-situ measurements. The bias is generally less than 0.05. The RMSE is approximately 0.14 when validating with total FAPAR measurements. However, the MODIS and MISR FAPAR products might overestimate at some sites. For example, Martinez et al. (2013) point out that MODIS shows a tendency to provide high values in cultivated areas and Mediterranean forest, such as Puéchabon. The MODIS FAPAR product may also have positive bias for very low FAPAR values. A similar overestimation problem is found in MISR FAPAR data as well, with a positive bias as large as 0.16 in broadleaf forests (Hu et al., 2007). In addition, unrealistically strong temporal variations are found in MODIS data, possibly because of severe cloud contamination during the wet season (Camacho et al., 2013). The MODIS FAPAR product tends to be more consistent with in-situ measurements in the dry season, linked to the absence of significant understory green vegetation, leaving the overlying evergreen woody vegetation as the sole vegetation layer (Pickett-Heaps et al., 2014). Regardless, the latest versions of the FAPAR products have higher levels of consistency than their previous versions, thanks to the continuously improved pre-processing of the products, including better calibration, clouds masks, etc. (Serbin et al., 2013).

6. Conclusions

This study aims at intercomparison and direct validation of five global FAPAR products, namely, MODIS, MERIS, MISR, SeaWiFS, and GEOV1 over different land cover types at the global, hemispheric and local scales. Absolute FAPAR values are on average in decreasing order of MISR, MODIS, GEOV1, SeaWiFS, and MERIS. The MISR and MODIS FAPAR products tend to agree well with each other and so do the MERIS and SeaWiFS FAPAR products, but the difference between the two groups could be as large as 0.1. The trends of the products agree better with each other in the Northern Hemisphere and globally than in the Southern Hemisphere. The trends of northern hemispheric FAPAR are close to those of global FAPAR over most of the land cover types, including grass, crop, shrubland, and broadleaf deciduous, needleleaf evergreen, and needleleaf deciduous forests. However, the conclusions from the northern hemispheric scale cannot be extended to the global scale for land covers such as savannahs and broadleaf evergreen forests, where seasonal patterns are obvious in the Northern Hemisphere but unnoticeable globally, because of the large contribution from the Southern Hemisphere over these two land covers. The differences between the products are consistent throughout the year over most of the land cover types, except over the forests. The possible reason could be traced to the different assumptions in the retrieval algorithms over forests and the differences between green and total FAPAR products due to tree trunks and branches absorption.

The MERIS, MODIS, MISR, and GEOV1 FAPAR products have an uncertainty of 0.14 validating with total FAPAR measurements, and 0.09 validating with green FAPAR measurements. The uncertainties of current satellite FAPAR products (within ± 0.1) are still unable to meet the threshold accuracy requirements stipulated by GCOS (± 0.05). Further improvements include combining multiple observations with reduced uncertainty and considering the scale difference between in-situ measurements and moderate resolution pixels.

Acknowledgements

The authors thank the AmeriFlux and VALERI PIs and staff for publishing the in-situ data (WWW1; WWW2). We thank the MODIS land product processing team at Oak Ridge National Laboratory Distributed Active Archive Center for the MODIS Collection 5 data (WWW3). The authors are thankful to the EOS MISR, ESA MERIS, and geoland2 GEOV1 land processing teams (WWW4; WWW5; WWW6). We would like to thank the SeaWiFS project and the Distributed Active Archive Center at the Goddard Space Flight Center for the production and distribution of the SeaWiFS data as well (WWW7). We thank the anonymous reviewers who provided helpful comments on the manuscript.

References

Baret, F., Hagolle, O., Geiger, B., Bicheron, P., Miras, B., Huc, M., Berthelot, B., Nino, F., Weiss, M., Samain, O., Roujean, J. L., & Leroy, M. (2007). LAI, fAPAR and fCover CYCLOPES global products derived from VEGETATION — Part 1: Principles of the algorithm. *Remote Sensing of Environment*, *110*, 275–286.

Baret, F., Weiss, M., Lacaze, R., Camacho, F., Makhmara, H., Pacholcyzk, P., & Smets, B. (2013). GEOV1: LAI and FAPAR essential climate variables and FCOVER global time series capitalizing over existing products. Part 1: Principles of development and production. *Remote Sensing of Environment*, *137*, 299–309.

Bonan, G. B., Oleson, K. W., Vertenstein, M., Levis, S., Zeng, X., Dai, Y., Dickinson, R. E., & Yang, Z. L. (2002). The land surface climatology of the community land model coupled to the NCAR community climate model. *Journal of Climate*, *15*, 3123–3149.

Camacho, F., Cemicharo, J., Lacaze, R., Baret, F., & Weiss, M. (2013). GEOV1: LAI, FAPAR essential climate variables and FCOVER global time series capitalizing over existing products. Part 2: Validation and intercomparison with reference products. *Remote Sensing of Environment*, *137*, 310–329.

D'Odorico, P., Gonsamo, A., Pinty, B., Gobron, N., Coops, N., Mendez, E., & Schaepman, M. E. (2014). Intercomparison of fraction of absorbed photosynthetically active radiation products derived from satellite data over Europe. *Remote Sensing of Environment*, *142*, 141–154.

Fensholt, R., Sandholt, I., & Rasmussen, M. S. (2004). Evaluation of MODIS LAI, fAPAR and the relation between fAPAR and NDVI in a semi-arid environment using in situ measurements. *Remote Sensing of Environment*, *91*, 490–507.

GCOS. (2011). *Systematic observation requirements for satellite-based data products for climate, 79–83.*

Gobron, N., Pinty, B., Aussedat, O., Chen, J. M., Cohen, W. B., Fensholt, R., Gond, V., Huemmrich, K. F., Lavergne, T., Melin, F., Privette, J. L., Sandholt, I., Taberner, M., Turner, D. P., Verstraete, M. M., & Widlowski, J. L. (2006). Evaluation of fraction of absorbed photosynthetically active radiation products for different canopy radiation transfer regimes: Methodology and results using Joint Research Center products derived from SeaWiFS against ground-based estimations. *Journal of Geophysical Research-Atmospheres*, *111*. http://dx.doi.org/10.1029/2005JD006511.

Gobron, N., Pinty, B., Aussedat, O., Taberner, M., Faber, O., Melin, F., Lavergne, T., Robustelli, M., & Snoeij, P. (2008). Uncertainty estimates for the FAPAR operational products derived from MERIS — Impact of top-of-atmosphere radiance uncertainties and validation with field data. *Remote Sensing of Environment*, *112*, 1871–1883.

Gobron, N., Pinty, B., Verstraete, M., & Govaerts, Y. (1999). The MERIS Global Vegetation Index (MGVI): Description and preliminary application. *International Journal of Remote Sensing*, *20*, 1917–1927.

Gobron, N., Pinty, B., Verstraete, M. M., & Widlowski, J. L. (2000). Advanced vegetation indices optimized for up-coming sensors: Design, performance, and applications. *IEEE Transactions on Geoscience and Remote Sensing*, *38*, 2489–2505.

Hanan, N. P., Burba, G., Verma, S. B., Berry, J. A., Suyker, A., & Walter-Shea, E. A. (2002). Inversion of net ecosystem CO_2 flux measurements for estimation of canopy PAR absorption. *Global Change Biology*, *8*, 563–574.

Hu, J. N., Su, Y., Tan, B., Huang, D., Yang, W. Z., Schull, M., Bull, M. A., Martonchik, J. V., Diner, D. J., Knyazikhin, Y., & Myneni, R. B. (2007). Analysis of the MISR LA/FPAR product for spatial and temporal coverage, accuracy and consistency. *Remote Sensing of Environment*, *107*, 334–347.

Huemmrich, K. F., Privette, J. L., Mukelabai, M., Myneni, R. B., & Knyazikhin, Y. (2005). Time-series validation of MODIS land biophysical products in a Kalahari woodland, Africa. *International Journal of Remote Sensing*, *26*, 4381–4398.

Kaminski, T., Knorr, W., Scholze, M., Gobron, N., Pinty, B., Giering, R., & Mathieu, P. P. (2012). Consistent assimilation of MERIS FAPAR and atmospheric CO_2 into a terrestrial vegetation model and interactive mission benefit analysis. *Biogeosciences*, *9*, 3173–3184.

Knyazikhin, Y., Martonchik, J. V., Diner, D. J., Myneni, R. B., Verstraete, M., Pinty, B., & Gobron, N. (1998). Estimation of vegetation canopy leaf area index and fraction of absorbed photosynthetically active radiation from atmosphere-corrected MISR data. *Journal of Geophysical Research-Atmospheres*, *103*, 32239–32256.

Liang, S., Li, X., & Wang, J. (2012). *Advanced Remote Sensing: Terrestrial Information Extraction and Applications.* Academic Press (ISBN 9780123859556).

Martinez, B., Camacho, F., Verger, A., Garcia-Haro, F. J., & Gilabert, M. A. (2013). Intercomparison and quality assessment of MERIS, MODIS and SEVIRI FAPAR products over the Iberian Peninsula. *International Journal of Applied Earth Observation and Geoinformation*, *21*, 463–476.

Maselli, F., Chiesi, M., Fibbi, L., & Moriondo, M. (2008). Integration of remote sensing and ecosystem modelling techniques to estimate forest net carbon uptake. *International Journal of Remote Sensing*, *29*, 2437–2443.

McCallum, A., Wagner, W., Schmullius, C., Shvidenko, A., Obersteiner, M., Fritz, S., & Nilsson, S. (2010). Comparison of four global FAPAR datasets over Northern Eurasia for the year 2000. *Remote Sensing of Environment*, *114*, 941–949.

Morton, D. C., Nagol, J., Carabajal, C. C., Rosette, J., Palace, M., Cook, B. D., Vermote, E. F., Harding, D. J., & North, P. R. J. (2014). Amazon forests maintain consistent canopy structure and greenness during the dry season. *Nature*, *506*, 221–224.

Myneni, R. B., Hoffman, S., Knyazikhin, Y., Privette, J. L., Glassy, J., Tian, Y., Wang, Y., Song, X., Zhang, Y., Smith, G. R., Lotsch, A., Friedl, M., Morisette, J. T., Votava, P., Nemani, R. R., & Running, S. W. (2002). Global products of vegetation leaf area and fraction absorbed PAR from year one of MODIS data. *Remote Sensing of Environment*, *83*, 214–231.

Myneni, R. B., Yang, W. Z., Nemani, R. R., Huete, A. R., Dickinson, R. E., Knyazikhin, Y., Didan, K., Fu, R., Juarez, R. I. N., Saatchi, S. S., Hashimoto, H., Ichii, K., Shabanov, N. V., Tan, B., Ratana, P., Privette, J. L., Morisette, J. T., Vermote, E. F., Roy, D. P., Wolfe, R. E., Friedl, M. A., Running, S. W., Votava, P., El-Saleous, N., Devadiga, S., Su, Y., & Salomonson, V. V. (2007). Large seasonal swings in leaf area of Amazon rainforests. *Proceedings of the National Academy of Sciences of the United States of America*, *104*, 4820–4823.

Olofsson, P., & Eklundh, L. (2007). Estimation of absorbed PAR across Scandinavia from satellite measurements. Part II: Modeling and evaluating the fractional absorption. *Remote Sensing of Environment*, *110*, 240–251.

Pickett-Heaps, C. A., Canadell, J. G., Briggs, P. R., Gobron, N., Haverd, V., Paget, M. J., Pinty, B., & Raupach, M. R. (2014). Evaluation of six satellite-derived Fraction of Absorbed Photosynthetic Active Radiation (FAPAR) products across the Australian continent. *Remote Sensing of Environment*, *140*, 241–256.

Seixas, J., Carvalhais, N., Nunes, C., & Benali, A. (2009). Comparative analysis of MODIS-FAPAR and MERIS-MGVI datasets: Potential impacts on ecosystem modeling. *Remote Sensing of Environment*, *113*, 2547–2559.

Serbin, S. P., Ahl, D. E., & Gower, S. T. (2013). Spatial and temporal validation of the MODIS LAI and FPAR products across a boreal forest wildfire chronosequence. *Remote Sensing of Environment*, *133*, 71–84.

Shabanov, N. V., Huang, D., Yang, W. Z., Tan, B., Knyazikhin, Y., Myneni, R. B., Ahl, D. E., Gower, S. T., Huete, A. R., Aragao, L., & Shimabukuro, Y. E. (2005). Analysis and optimization of the MODIS leaf area index algorithm retrievals over broadleaf forests. *IEEE Transactions on Geoscience and Remote Sensing*, *43*, 1855–1865.

Steinberg, D. C., Goetz, S. J., & Hyer, E. J. (2006). Validation of MODIS F-PAR products in boreal forests of Alaska. *IEEE Transactions on Geoscience and Remote Sensing*, *44*, 1818–1828.

Tao, X., Liang, S., & He, T. (2015). *Estimation of fraction of absorbed photosynthetically active radiation from multiple satellite data: Model development and validation.* Remote Sensing of Environment (in review).

Tao, X., Yan, B., Wang, K., Wu, D., Fan, W., Xu, X., & Liang, S. (2009). Scale transformation of leaf area index product retrieved from multi-resolution remotely sensed data: Analysis and case studies. *International Journal of Remote Sensing*, *30*, 5383–5395.

Tian, Y., Dickinson, R. E., Zhou, L., Zeng, X., Dai, Y., Myneni, R. B., Knyazikhin, Y., Zhang, X., Friedl, M., Yu, I. I., Wu, W., & Shaikh, M. (2004). Comparison of seasonal and spatial variations of leaf area index and fraction of absorbed photosynthetically active radiation from Moderate Resolution Imaging Spectroradiometer (MODIS) and Common Land Model. *Journal of Geophysical Research-Atmospheres*, *109*. http://dx.doi.org/10.1029/2003JD003777.

Turner, D. P., Ritts, W. D., Cohen, W. B., Maeirsperger, T. K., Gower, S. T., Kirschbaum, A. A., Running, S. W., Zhao, M. S., Wofsy, S. C., Dunn, A. L., Law, B. E., Campbell, J. L., Oechel, W. C., Kwon, H. J., Meyers, T. P., Small, E. E., Kurc, S. A., & Gamon, J. A. (2005). Site-level evaluation of satellite-based global terrestrial gross primary production and net primary production monitoring. *Global Change Biology*, *11*, 666–684.

Vina, A., & Gitelson, A. A. (2005). New developments in the remote estimation of the fraction of absorbed photosynthetically active radiation in crops. *Geophysical Research Letters*, *32*.

Wang, Y., Tian, Y., Zhang, Y., El-Saleous, N. Z., Knyazikhin, Y., Vermote, E. F., & Myneni, R. B. (2001). Investigation of product accuracy as a function of input and model uncertainties: Case study with SeaWiFS and MODIS LAI/FPAR algorithm. *Remote Sensing of Environment*, *78*, 299–313.

Weiss, M., Baret, F., Garrigues, S., & Lacaze, R. (2007). LAI and fAPAR CYCLOPES global products derived from VEGETATION. Part 2: validation and comparison with MODIS collection 4 products. *Remote Sensing of Environment*, *110*, 317–331.

Xu, X., Fan, W., & Tao, X. (2009). The spatial scaling effect of continuous canopy leaves area index retrieved by remote sensing. *Science in China Series D-Earth Sciences*, *52*, 393–401.

Yang, W. Z., Huang, D., Tan, B., Stroeve, J. C., Shabanov, N. V., Knyazikhin, Y., Nemani, R. R., & Myneni, R. B. (2006). Analysis of leaf area index and fraction of PAR absorbed by vegetation products from the terra MODIS sensor: 2000-2005. *IEEE Transactions on Geoscience and Remote Sensing*, *44*, 1829–1842.

Zhang, Q., Xiao, X., Braswell, B., Linder, E., Baret, F., & Moore, B., III (2005). Estimating light absorption by chlorophyll, leaf and canopy in a deciduous broadleaf forest using MODIS data and a radiative transfer model. *Remote Sensing of Environment*, *99*, 357–371.

WWW Sites

WWW1. (d). The VALERI validation data. http://w3.avignon.inra.fr/valeri/fic_htm/database/main.php

WWW2. (d). The AmeriFlux validation data. http://ameriflux.ornl.gov/

WWW3. (d). The MODIS Collection 5 data. http://ladsweb.nascom.nasa.gov/data/search.html

WWW4. (d). The MISR data. http://l0dup05.larc.nasa.gov/MISR/cgi-bin/MISR/main.cgi

WWW5. (d). The geoland2 GEOV1 product. http://land.copernicus.eu/global/products/FAPAR

WWW6. (d). The MERIS data. https://earth.esa.int/web/guest/data-access/browse-data-products

WWW7. (d). The SeaWiFS data. http://fapar.jrc.ec.europa.eu/WWW/Data/Pages/FAPAR_Download/FAPAR_Download.php#a_dataTable